# 2.B Laser Ionization of Noble Gases by Coulomb Barrier Suppression

## Introduction

The ionization of atoms and ions in high-intensity laser fields allows a study of atomic structure under extreme conditions. The electric field of the laser can approach or even exceed the electric field binding an electron to a nucleus. At even higher laser intensities, electron motion in the laser field can become relativistic.

We have studied the ionization of five noble gases with 1.053-μm, 1-ps laser pulses[1] using the tabletop terawatt laser ($T^3$) (see Ref. 2), developed at LLE. Experimentally measured intensities ranging from mid-$10^{13}$ W/cm$^2$ to mid-$10^{16}$ W/cm$^2$ were used with charge states up to $He^{2+}$, $Ne^{6+}$, $Kr^{8+}$, $Ar^{8+}$, and $Xe^{12+}$ observed. It was found that the "appearance" or "threshold" intensity (intensity at which ionization of a particular charge state commences) was a function of both the ionization potential and the charge of the ionic state. The ionization occurred completely in the tunneling regime and was accurately predicted by a simple model of Coulomb barrier suppression due to the laser electric field [barrier suppression ionization (BSI)].[1]

Experiments involving the interaction of atoms with intense laser fields have traditionally been divided into two regimes: multiphoton and tunneling. In the former, laser ionization can be described by perturbation theory, while in the latter ionization can be described as an ac tunneling process. These regions can be quantitatively separated by introducing the Keldysh $\gamma$ parameter[3]

$$\gamma = \sqrt{\frac{E}{2\Phi}}\ , \tag{1}$$

where $E$ is the ionization potential of the atom or ion and $\Phi$ is the ponderomotive potential of the laser,

$$\Phi(\mathrm{eV}) = \frac{e^2\mathcal{E}^2}{4m\omega^2} 9.33\times10^{-14} \times I(W/\mathrm{cm}^2) \times \lambda^2(\mu\mathrm{m}), \tag{2}$$

where $\mathcal{E}$ is the laser electric field. In the multiphoton regime, $\gamma > 1$, the laser field can be treated perturbatively while in the tunneling regime, $\gamma < 1$, the laser field is treated quasistatically.

Most laser-induced ionization experiments performed to date have observed ion production in the multiphoton regime.[4–9] Work in the tunneling regime has been, up to now, confined to 10-μm-wavelength $CO_2$ lasers.[10–12] Thus, these results represent the first observations of ionization in the tunneling regime for near-visible wavelengths, and the highest charge states observed in this regime.

We will first discuss the laser characteristics and the experimental apparatus. A presentation of the data and a comparison to the BSI theory follows.

**Experiments**

The laser used for these experiments is an Nd:glass laser based on the concept of chirped pulse amplification and compression (CPAC).[2] The laser is operated at the fundamental wavelength of 1.053 μm, with a nominal pulse width of 1 ps and a bandwidth of ~20 Å. Using f/5 optics (20-cm-focal-length lens) intensities up to mid-$10^{16}$ W/cm$^2$ were obtained. The intensity is known with a relative shot-to-shot uncertainty of 25% and an absolute uncertainty of a factor of ~2.

The experiment is set up to detect noble gas ions produced by very intense laser fields. A single gas, or mixture of gases, is introduced into a vacuum chamber by means of a leak valve. The target gas (He, Ne, Ar, Kr, and/or Xe) uniformly back-fills the chamber to a pressure of typically $5 \times 10^{-6}$ Torr. A liquid-nitrogen-trapped diffusion pump is used to obtain a background pressure of $1 \times 10^{-8}$ Torr that is sufficient to eliminate almost all impurity signals from our ion spectra.

The ion spectra are obtained with a standard time-of-flight spectrometer that has an extraction field of 800 V/cm and a field-free drift length of 30 cm. The ions are detected with a dual microchannel plate (MCP) operated at 1000 V/plate that gives a total signal gain of ~$10^6$. The spectra are recorded with a digitizing oscilloscope that allows resolution of charge states up to $Xe^{13+}$.

After the spectra are stored, the individual ion peaks are integrated to determine the number of ions detected in each charge state. These values are then plotted versus the laser intensity for that shot. The graphs, shown in Figs. 41.34(a) and 41.34(b), plot the number of ions detected versus laser intensity for xenon and neon. The solid curves are from theoretical calculations and will be discussed in the following section. For clarity, data that reflect detector saturation effects have been removed from these graphs.

The appearance intensity of each of the various charge states seen is defined as the lowest intensity at which that charge state can be detected above the background detector noise. Since the slope of the data curves is very steep for low ion number, the exact choice of the number of ions detected is unimportant. A value of 10 ions detected has been chosen to determine the appearance intensities. A comparison of the appearance intensities for the various gases demonstrates a significant atomic species dependence on the ionization rates as can be seen in Fig. 41.35. All charge states detected were produced in the regime of $\gamma < 1$, which indicates that we are operating exclusively in the tunneling regime.

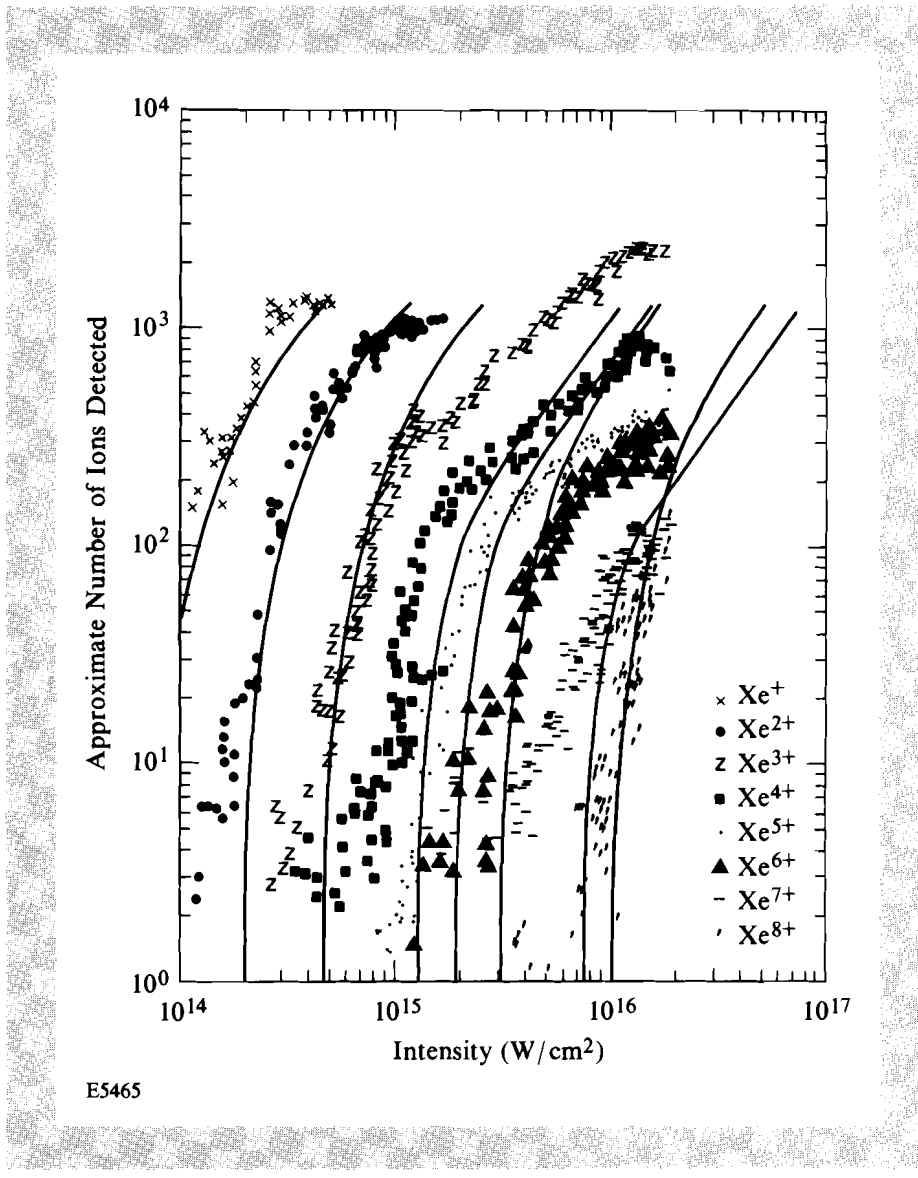


Fig. 41.34(a)
Xenon ion-production rate as a function of laser intensity. The theoretical curves are from BSI theory with no shift in intensity. ($P = 5 \times 10^{-6}$ Torr).

### Barrier Suppression Ionization

A simple one-dimensional model of ionization consists of a superposition of the Coulomb potential with a static electric field.[13] The laser electric field suppresses the Coulomb field thereby creating a barrier over which an electron can escape. The resulting potential is written as

$$V(x) = -\frac{Ze^2}{|x|} - e\,\mathcal{E}x\,. \tag{3}$$

This potential has a relative maximum located at $x_{max}$ that can easily be found by setting $\partial V(x)/\partial x = 0$ and solving for $x_{max}$. Equating $V(x_{max})$ to the

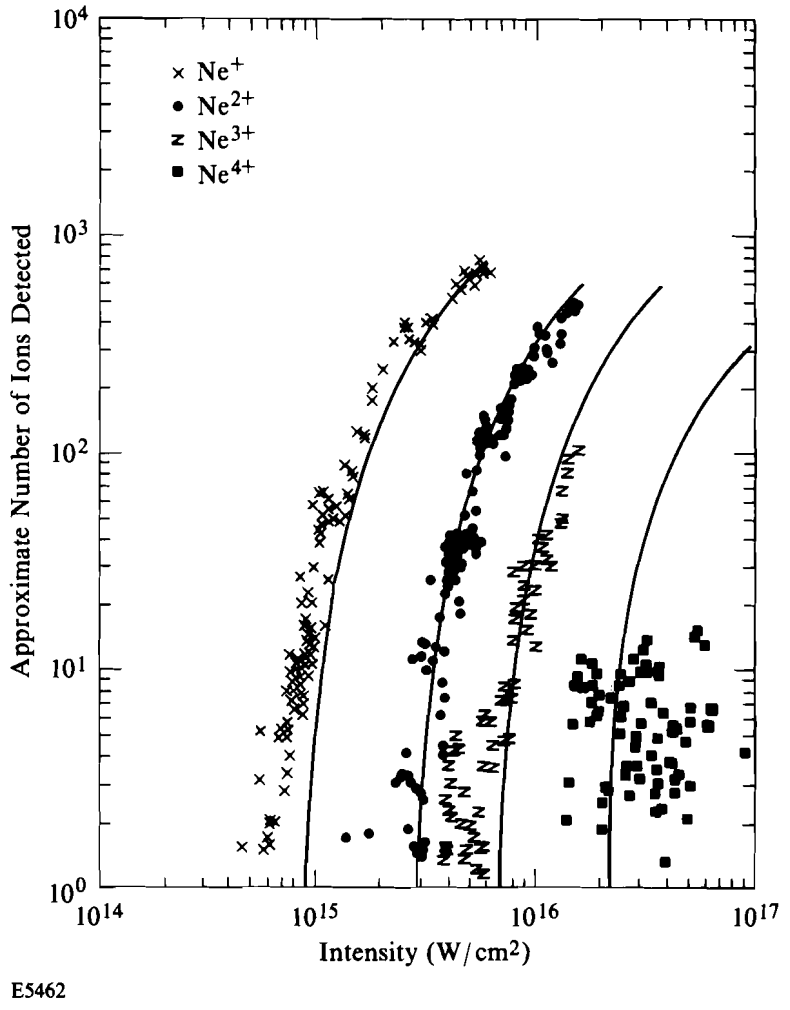


Fig. 41.34(b)
Neon ion-production rate as a function of laser intensity. The theoretical curves are from BSI theory with no shift in intensity. ($P = 2.5 \times 10^{-6}$ Torr).

ionization potential ($E$) of the atom or ion permits us to find the critical electric field that is necessary to allow the bound electron to escape without tunneling. The critical electric field is

$$\mathcal{E}^2 = \frac{E^4}{16e^2Z^2} \cdot \tag{4}$$

Setting the magnitude of the laser electric field equal to this critical field strength results in a laser intensity that can be considered to be the appearance intensity

$$I_{\text{app}} = \frac{cE^4}{128\pi e^6 Z^2} \cdot \tag{5}$$

In a Coulombic system, the ionization potential is dependent on the ionic charge $Z$ and the principal quantum number $n$: $E = (m_e Z^2\alpha^2c^2)/(2n^2)$. However, for the calculations used here, electron-shielding effects are accounted for by using values of $E$ that have been determined either experimentally or by use of more complicated calculations than those given in the Bohr model. Appearance intensities calculated in this manner are compared to the experimentally determined ones in Fig. 41.36. In all cases the theory and experiment agree within the experimental uncertainties.

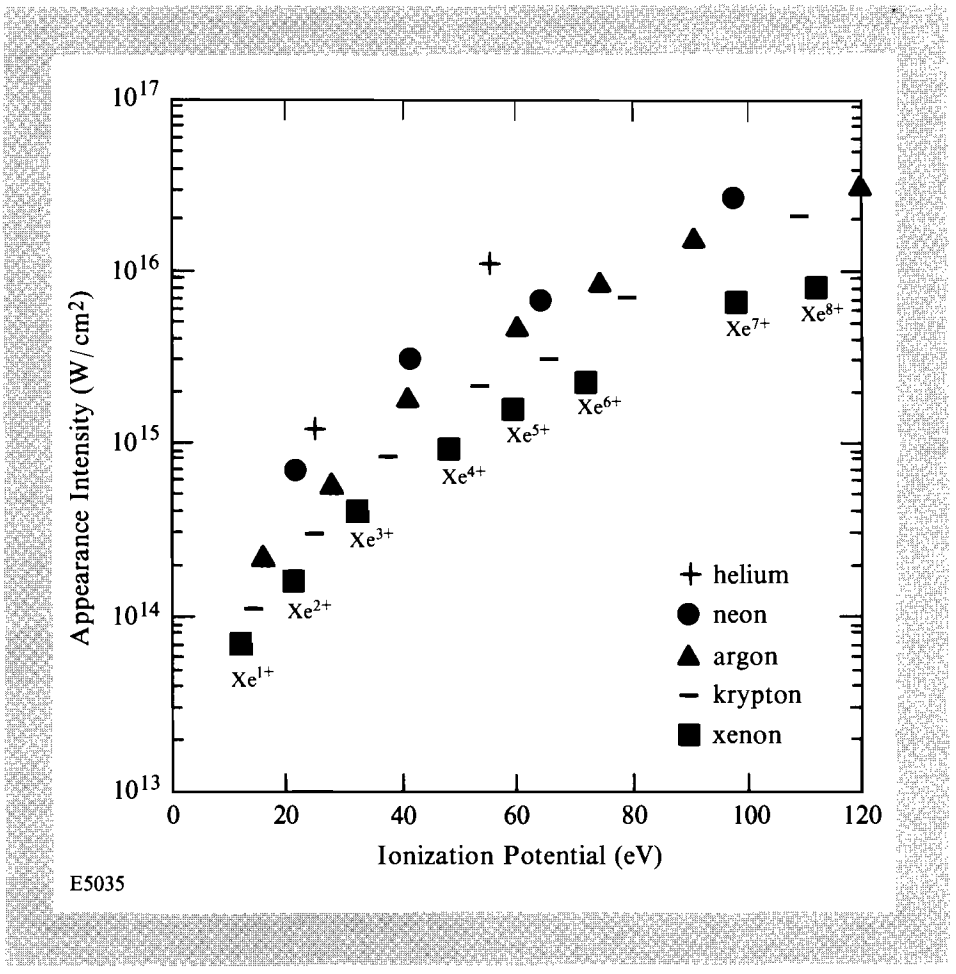


Fig. 41.35
Appearance intensity of each charge state versus the sequential ionization potential showing a clear species dependence present.

In addition to comparing appearance intensities, theoretical ion-production curves are obtained by integrating the coupled rate equations for the number of ions in each charge state. The spatial and temporal dependence of the intensity, and consequently of the ionization rates, is also accounted for in the calculation. The integration is performed by finding the volume of each iso-intensity shell and then propagating a laser pulse through that volume. The number of particles in each shell is conserved so saturation effects are

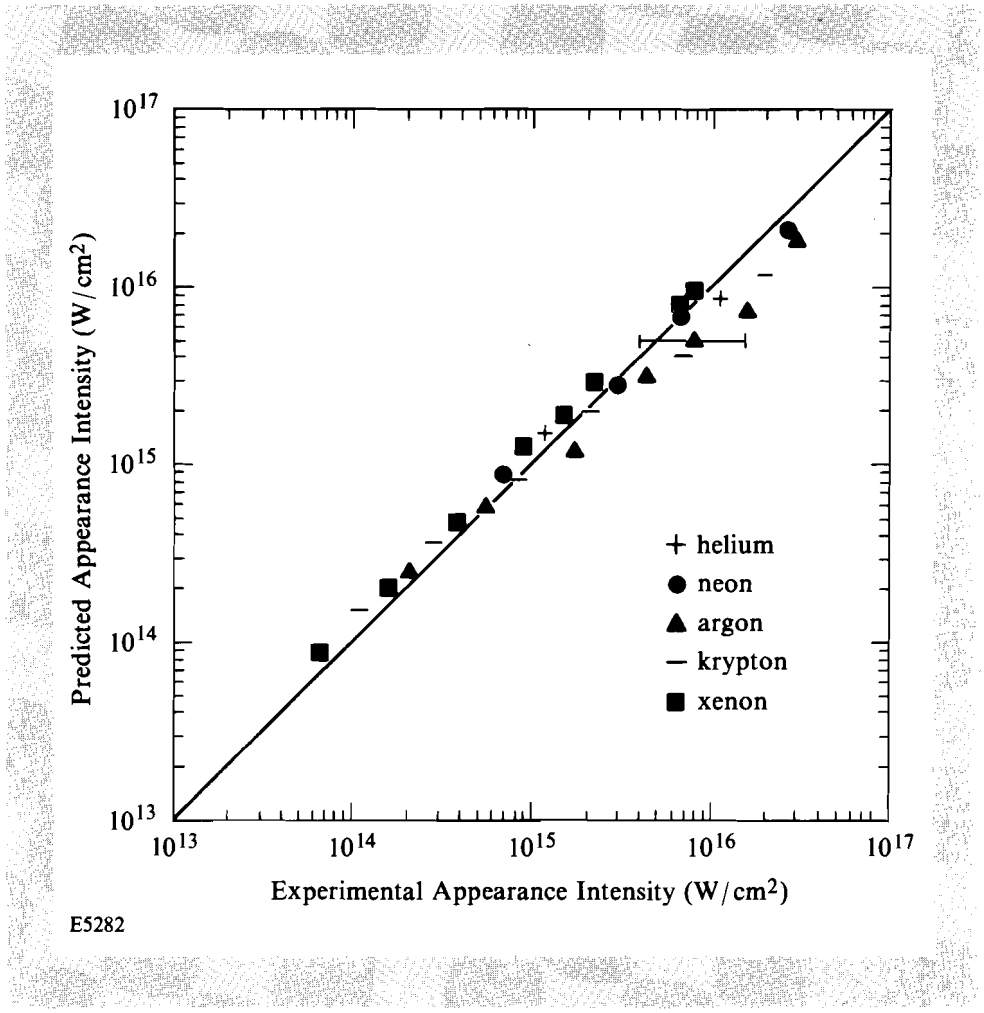


Fig. 41.36
Comparison of measured appearance intensities and those obtained from BSI theory [Eq. (5)]. A typical experimental error bar is shown.

accounted for. The intensity distribution is modeled as temporally Lorentzian and spatially Gaussian.[14] The volume of an iso-intensity shell is

$$\text{Volume} = \frac{\pi z_R w_o^2}{2}\left\{\frac{4(c_1 - c_2)}{3} + \frac{2\left(c_1^3 - c_2^3\right)}{9} - \frac{4}{3}\left[\tan^{-1}(c_1) - \tan^{-1}(c_2)\right]\right\}, \tag{6}$$

where $w_o$ is the $1/e$ diameter of the focal spot, $z_R = \pi w_o^2 / \lambda$ is the Rayleigh range of the focus, and

$$c_j = R\sqrt{(I_o - I_j)/I_j}$$

with $I_o$ being the peak laser intensity and $I_j$ the intensity of shell $j$. The calculation assumes only sequential ionization occurs.

The ion spectra are calculated for BSI theory by assuming that the ionization probability is unity for $I \geq I_{app}$ and zero for $I < I_{app}$. The resulting BSI theory curves shown in Fig. 41.34 use a one-parameter fit, this being the shift in the vertical scale that simply accounts for spectrometer efficiency. There has been no shift along the intensity scale for theoretical curves shown in Fig. 41.34; thus, these are effectively zero-parameter fits to the ionization. As can be seen, the agreement is excellent.

**Summary/Discussion**

In summary, we present results of high-intensity laser ionization of noble gases. It is found that for a 1-ps laser pulse at $\lambda = 1.053$ μm, the ionization rates are strongly species dependent, unlike results obtained with a 1-ps, 586-nm laser.[7] Additionally, all ion production occurs in the tunneling regime ($\gamma < 1$), contrary to results obtained with a 50-ps laser pulse at the same wavelength that clearly shows ion production occurring in the multiphoton regime.[9]

The measured ion production is well predicted by a Coulomb barrier suppression ionization theory.

ACKNOWLEDGMENT

This work was supported by the National Science Foundation Grant PHY-8822730. Additional support was provided by the U.S. Department of Energy Division of Inertial Fusion under agreement No. DE-FC03-85DP40200 and by the Laser Fusion Feasibility Project at the Laboratory for Laser Energetics, which has the following sponsors: Empire State Electric Energy Research Corporation, New York State Energy Research and Development Authority, Ontario Hydro, and the University of Rochester.

REFERENCES

1. S. Augst, D. Strickland, D. D. Meyerhofer, S. L. Chin, and J. H. Eberly, *Phys. Rev. Lett.* **63**, 2212 (1989).
2. P. Maine, D. Strickland, P. Bado, M. Pessot, and G. Mourou, *IEEE J. Quantum Electron.* **QE-24**, 398 (1988).
3. L. V. Keldysh, *Sov. Phys. JETP* **20**, 1307 (1965).
4. T. S. Luk *et al.*, *Phys. Rev. A* **32**, 214 (1985).
5. C. K. Rhodes, *Phys. Scr.* **T17**, 193 (1987).
6. S. L. Chin, C. Rolland, P. B. Corkum, and P. Kelly, *Phys. Rev. Lett.* **61**, 153 (1988).
7. M. D. Perry, O. L. Landen, A. Szöke, and E. M. Campbell, *Phys. Rev. A* **37**, 747 (1988).
8. M. D. Perry, A. Szöke, O. L. Landen, and E. M. Campbell, *Phys. Rev. Lett.* **60**, 1270 (1988).
9. A. L'Huillier, L. A. Lompré, G. Mainfray, and C. Manus, *J. Phys. B* **16**, 1363 (1983).
10. F. Yergeau, S. L Chin, and P. Lavigne, *J. Phys. B* **20**, 723 (1987).

11. S. L. Chin, W. Xiong, and P. Lavigne, *J. Opt. Soc. Am. B* **4**, 853 (1987).

12. S. L. Chin and W. Xiong, *Fundamentals of Laser Interactions II*, edited by F. Ehlotzky (Springer-Verlag, Berlin, 1989), p. 80.

13. BSI is a simplified version of work done by M. Brewczyk and M. Gajda, *J. Phys. B* **21**, L383 (1988); E. J. Valeo, S. M. Susskind, C. R. Oberman, and I. B. Berstein, *Bull. Am. Phys. Soc.* **34**, 2099 (1989).

14. D. T. Strickland, Ph.D. thesis, University of Rochester, 1989.